Relevance of memory in minority games

Damien Challet[1] and Matteo Marsili[2]
[1]*Institut de Physique Théorique, Université de Fribourg, CH-1700 Fribourg, Switzerland*
[2]*Istituto Nazionale per la Fisica della Materia (INFM), Trieste-SISSA Unit, Via Beirut 2-4, Trieste I-34014, Italy*
(Received 12 April 2000)

By considering diffusion on De Bruijn graphs, we study in detail the dynamics of the histories in the minority game, a model of competition between adaptative agents. Such graphs describe the structure of the temporal evolution of M bit strings, each node standing for a given string, i.e., a history in the minority game. We show that the frequency of visit of each history is not given by $1/2^M$ in the limit of large M when the transition probabilities are biased. Consequently, all quantities of the model do significantly depend on whether the histories are real or uniformly and randomly sampled. We expose a self-consistent theory of the case of real histories, which turns out to be in very good agreement with numerical simulations.

PACS number(s): 02.50.Le, 05.40.−a, 64.60.Ak, 89.90.+n

I. INTRODUCTION

The minority game (MG) [1,2] has been designed as the most drastic possible simplification of Arthur's El Farol's bar problem [3]. It is believed to capture some essential and general features of the competition between adaptative agents, which is found, for instance, in financial markets. In this model, agents have to make at each time step one of two decisions; they share a common piece of information $\mu \in \{0, \ldots, P-1\}$ that encodes the state of the world, use it to make their choice, and those who happen to be in the minority are rewarded. In its original formulation, the piece of information is the binary encoding of the M last winning choices; hence $P=2^M$. Hence, the dynamics of μ is coupled to the dynamics of agents.

Cavagna [4] claimed that all quantities of the system ''are completely independent from the memory of the agents.'' This means that replacing the dynamics of μ induced by agents by a random history μ drawn at random at each time step, one finds the same results. While this statement has turned out to be wrong for many extensions of the MG [5–8], it has been helpful as a first approximation for the analytical understanding of the standard MG: an exact solution for random histories has been found in the ''thermodynamic'' limit [7,8]. Interestingly, this solution shows that all quantities depend on the frequencies $\{\rho^\mu\}$ of the visit of histories. The random history case is recovered if $\rho^\mu = 1/P$, but in the real dynamics of the MG the distribution ρ^μ is determined by the behavior of agents (indeed modifying the behavior of agents may have strong effects on ρ^μ as shown in Refs. [7,8]). It turns out that the frequencies ρ^μ are not uniform for all parameters of the MG.

In this paper we study quantitatively this problem. The first step is to characterize the properties of the dynamics of real histories, which amounts to studying randomly biased diffusion on De Bruijn graphs. Depending on the asymmetry of the bias, we quantify the deviation $\delta\rho^\mu = \rho^\mu - 1/P$ from the uniform distribution. Then we move to the MG and quantify the bias which agents induce on the dynamics of μ in the asymmetric phase. Using a simple parametrization of ρ^μ which is inferred from numerical data, we generalize the calculations of Refs. [7,8]. This leads to a self-consistent equation between the asymmetry of the game and the diffusion bias, which we can solve. The results are in excellent agreement with numerical simulations and show a systematic deviation from the random history MG. Hence, our conclusion is that, even though the random history MG is qualitatively similar to the original MG, memory is actually not irrelevant, and one can quantify the difference between the two cases.

II. DE BRUIJN GRAPHS

Let us begin with the definition of some elementary concepts. A binary sequence $\mu(t)$ of length M consists of M ordered elements $\{b(t-M), \ldots, b(t-1)\}$ where b is a letter belonging to the alphabet $\{0,1\}$. $\mu(t+1)$ is obtained by adding $b(t)$ to the right of $\mu(t)$ and erasing $b(t-M)$. Thus, for a given $\mu(t)$, there are two possible $\mu(t+1)$, which we call ''next neighbors.'' This updating rule defines the De Bruijn graph [9] of order M (see Fig. 1 for an example).

Let G be the $P \times P$ adjacency matrix of the De Bruijn graph of order M. If we adopt the convention that its elements are indiced by the decimal value of the binary strings, that is, $\mu = 0, \ldots, P-1$,

$$G_{\mu,\nu} = \delta_{[2\mu \% P],\nu} + \delta_{[2\mu \% P]+1,\nu}, \tag{1}$$

where $A\%B$ stands for the remainder of the division of B by A and $\delta_{i,j}$ is the Kronecker symbol. The adjacency matrix for $M=3$ is

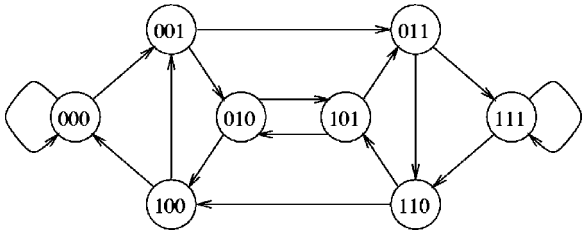

FIG. 1. De Bruijn graph of order 3.

$$G=\begin{pmatrix}1&1&0&0&0&0&0&0\\0&0&1&1&0&0&0&0\\0&0&0&0&1&1&0&0\\0&0&0&0&0&0&1&1\\1&1&0&0&0&0&0&0\\0&0&1&1&0&0&0&0\\0&0&0&0&1&1&0&0\\0&0&0&0&0&0&1&1\end{pmatrix}. \tag{2}$$

III. UNBIASED DIFFUSION

The unbiased diffusion is defined as follows: a particle moves on the directed De Bruijn graph G, and at each time step t, it jumps with equal probability to one of the next neighbors of the vertex it stands on at this time. Thus the transition probability matrix is $W_0=G/2$. In the long run, the fraction of time spent on vertex ν is given by $[(W_0)^\infty]_{0,\nu}$. It can be seen (see Appendix A) that

$$[(W_0)^k]_{\mu,\nu}=\frac{1}{2^k}\sum_{n=0}^{2^k-1}\delta_{[2^k\mu\%P]+n,\nu}. \tag{3}$$

In particular, $(W_0^{M+k})_{\mu,\nu}=1/P$ for all $k\geqslant 0$ that is, all strings μ are visited with the same frequency $\rho^\mu=1/P$.

In order to have a intuitive feeling of those graphs, we write them for $M=3$:

$$W_0^2=\frac{1}{4}\begin{pmatrix}1&1&1&1&0&0&0&0\\0&0&0&0&1&1&1&1\\1&1&1&1&0&0&0&0\\0&0&0&0&1&1&1&1\\1&1&1&1&0&0&0&0\\0&0&0&0&1&1&1&1\\1&1&1&1&0&0&0&0\\0&0&0&0&1&1&1&1\end{pmatrix},$$

$$W_0^3=W_0^4=W_0^5=\cdots=\frac{1}{8}\begin{pmatrix}1&1&1&1&1&1&1&1\\1&1&1&1&1&1&1&1\\1&1&1&1&1&1&1&1\\1&1&1&1&1&1&1&1\\1&1&1&1&1&1&1&1\\1&1&1&1&1&1&1&1\\1&1&1&1&1&1&1&1\\1&1&1&1&1&1&1&1\end{pmatrix}. \tag{4}$$

IV. RANDOMLY BIASED DIFFUSION

The perturbations are introduced by adding a term to the transition probabilities matrix $W_\epsilon=W_0+\epsilon W_1$ where ϵ quantifies the asymmetry and W_1 contains the disorder ξ:

$$(W_1)_{\mu,\nu}=(-1)^\nu\xi_\mu(W_0)_{\mu,\nu}, \tag{5}$$

where the ξ are drawn independently from the probability distribution function (PDF) $P(\xi)=1/2\delta(\xi-1)+1/2\delta(\xi+1)$ and the $(-1)^\nu$ comes from the normalization of the perturbed probabilities. We are looking for the stationary transition probabilities, i.e., W_ϵ^∞, such that $W_\epsilon^\infty=\lim_{k\to\infty}(W_\epsilon)^k$. It exists since W_ϵ is a bounded operator. Its formal series expansion in ϵ is denoted by $W_\epsilon^\infty=\Sigma_{k\geqslant 0}\epsilon^k W_k^\infty$ where W_0^∞ is a matrix all of whose coefficients are equal to $1/P$ (see above). The relationship $W_\epsilon^\infty=W_\epsilon^\infty W_\epsilon$ provides the recurrence

$$W_k^\infty=W_k^\infty W_0+W_{k-1}^\infty W_1. \tag{6}$$

Since $W_k^M W_0^\infty=0$, we iterate this equation $m-1$ times by replacing W_k^∞ with $W_k^\infty W_0+W_{k-1}^\infty W_1$ on the right-hand side (RHS), yielding

$$W_k^\infty=W_{k-1}^\infty W_1 V=W_0^\infty[W_1V]^k, \tag{7}$$

where $V=\Sigma_{c=0}^{M-1}(W_0)^c$. At this point, it is useful to remark that multiplying a matrix on the left by W_0^∞ is equivalent to averaging its columns:

$$(W_0^\infty A)_{\mu,\nu}=\sum_{a=0}^{P-1}(W_0^\infty)_{\mu,a}A_{a,\nu}=\frac{1}{P}\sum_{a=0}^{P-1}A_{a,\nu}$$
$$=(\text{average of the }\ \nu\text{th column of})A; \tag{8}$$

thus the matrices W_k^∞ consist of averages of columns of $(W_1V)^k$. Therefore, $(W_k^\infty)_{\mu,\nu}$ is the kth order correction to the frequency of vertex ν, which will be called $\rho_{(k)}^\nu$ in the following. Note that $\langle\rho_{(k)}^\nu\rangle_\xi=0$ for all $k\geqslant 1$. The square root of the second moment of $\rho_{(k)}^\nu$ averaged over the disorder gives an indication of the typical value of $\rho_{(k)}^\nu$. In Appendix B we obtain the approximation

$$\langle||\rho_{(k)}||^2\rangle_\xi\sim\frac{(1-1/P)^k}{P}, \tag{9}$$

which is exact for the first order perturbation. Therefore $\rho_{(k)}^\nu$ is of the same order as the unperturbed $\rho_{(0)}^\nu$; thus it cannot be neglected. Figure 2 shows that the behavior predicted by Eq. (9) is indeed correct for large P.

Finally, one can estimate the second moment of ρ^ν. If one supposes that the perturbations at different orders are independent, one obtains

$$\Delta\rho^2=\frac{1}{P}\sum_{\nu=0}^{P-1}[\langle[\rho^\nu]^2\rangle_\xi-\langle\rho^\nu\rangle_\xi^2]$$
$$\simeq\frac{1}{P^2}\left[\frac{1}{1-(1-1/P)\epsilon^2}-1\right]$$
$$\simeq\frac{1}{P^2}\frac{\epsilon^2}{1-\epsilon^2}. \tag{10}$$

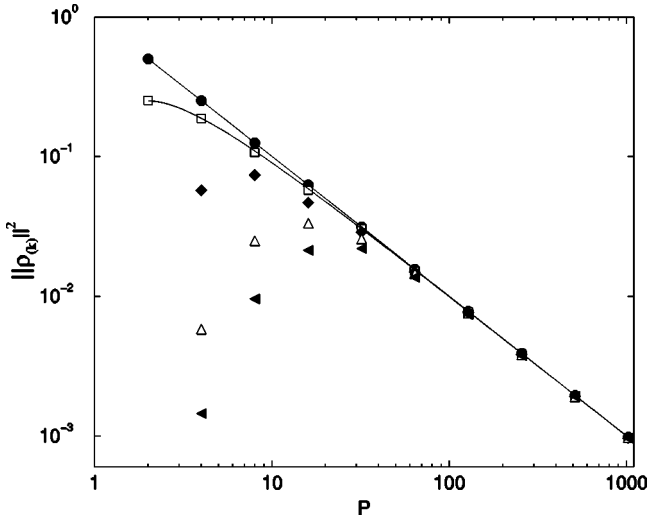

FIG. 2. Squared norms of $\rho_{(k)}$ for $k=0,\ldots,4$ (circles, squares, diamonds, open triangles, and solid triangles) (average over 500 samples). They decrease as $1/P$ for large P. The solid lines are exact theoretical predictions.

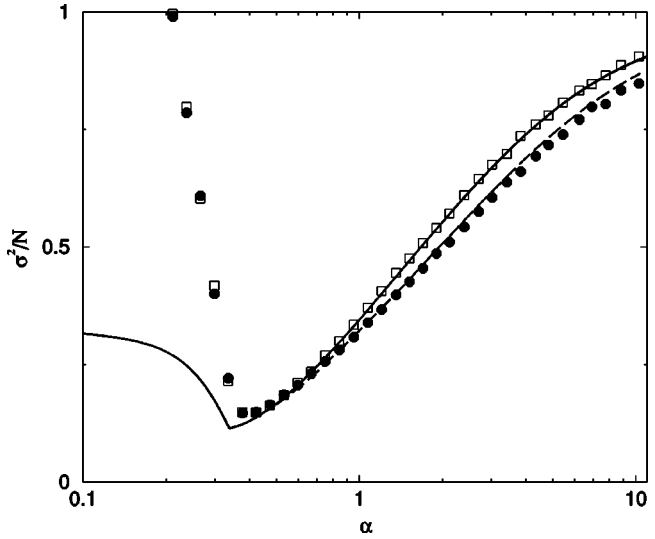

FIG. 3. Comparison between the fluctuations of the MG with uniformly sampled (squares) and real (circles) histories. In the symmetric phase, these are equal whereas they differ significantly in the asymmetric phase. Dashed and solid lines are corresponding theoretical predictions; they overlap in the symmetric phase ($M=8$, $S=2$, $300P$ iterations, average over 200 samples).

V. APPLICATION TO THE MG

Let us first define the game[1]: The MG consists of N agents trying to be at each time step in the minority. Each agent has S strategies or lookup tables $a_{i,s}$, $s=1,\ldots,S$, and dynamically assigns a score to each of them. At each time step t, the system's history $\mu(t)$ is made available to all agents; the latter use their best strategy[2] $s_i(t)$ to make the decision $a^{\mu}_{i,s_i(t)}(t)=+1$ or -1 and a market maker sums up all decisions into the aggregate quantity $A(t)=\Sigma_{i=1}^{N} a^{\mu}_{i,s_i(t)}(t)$.

Macroscopic quantities of interest include the temporal averages of the $A(t)$ conditional to $\mu(t)=\mu$, for all μ, denoted by $\langle A^{\mu}\rangle$. The MG undergoes a second order phase transition with symmetry breaking as the control parameter $\alpha=P/N$ is varied [10,11]: the system is in the symmetric phase ($\langle A^{\mu}\rangle=0$ for all μ) if $\alpha<\alpha_c$ and it is in the asymmetric phase for $\alpha>\alpha_c$. One convenient order parameter is[3] $H=\overline{\langle A\rangle^2}$: it is equal to zero in the symmetric phase, and grows monotonically with α in the asymmetric phase [11] (see Fig. 4). One other relevant macroscopic quantity is the fluctuations $\sigma^2=\overline{\langle A^2\rangle}$ which quantifty the performance of the agents [8,10–12].

Before doing any analytic calculations, it is worth looking at Fig. 3 and 4 which clearly show that Cavagna's assertion is right as long as the system is in the symmetric phase. Indeed, if $\langle A^{\mu}\rangle=0$, the transition probabilities from μ to its next neighbors are unbiased; that is, $\epsilon^{\mu}=0$. Therefore in the symmetric phase, where $\langle A^{\mu}\rangle=0$ for all μ, the frequencies of visit are uniform $\rho^{\mu}=1/P$. Accordingly, numerical simulations show that these quantities collapse on the same curve.

As α increases, the critical point is crossed, and $\langle A^{\mu}\rangle\neq 0$ for some μ. The dynamics of the history is biased on all such histories and consequently all macroscopic quantities are significantly different: both σ^2/N and H/N are lower for real histories than for uniformly sampled histories. This can be understood by the facts that σ^2/N and H are increasing functions of α and that the biases on the De Bruijn graph of histories reduce the effective number of histories that can be defined as $2^{-\overline{\log_2 \rho}}$: in other words, the effective α of the MG with real histories is smaller than that of the MG with uniform histories. This explanation is indeed confirmed by Fig. 5; this shows the fraction of frozen agents[4] ϕ which is a decreasing function of α in the asymmetric phase. As expected from the above argument, ϕ of the MG with real histories is larger than that of the MG with uniformly sampled histories.

The bias ϵ^{μ} on a particular history can be estimated for large N: in this limit A^{μ} is a Gaussian variable with average $\langle A^{\mu}\rangle$ and variance $\langle (A^{\mu})^2\rangle-\langle A^{\mu}\rangle^2$, leading to

$$\epsilon^{\mu}=\langle \mathrm{sgn}(A^{\mu})\rangle \simeq \epsilon^{\mu}_{th}=\mathrm{erf}\left(\sqrt{\frac{\langle A^{\mu}\rangle^2}{2[\langle (A^{\mu})^2\rangle-\langle A^{\mu}\rangle^2]}}\right). \tag{11}$$

Figure 6 confirms the validity of Eq. (11). The figure also shows that ϵ^{μ} are unevenly distributed and they are not equal even if the system is deep in the asymmetric phase ($\alpha\simeq 8.5$ in this figure). Indeed, as a function of μ, $\langle A^{\mu}\rangle$ is a random variable with average 0 and variance H, which is an increasing function of α. Since we studied the diffusion of perturbed graphs with only one parameter ϵ, we have to map all ϵ^{μ} onto a scalar quantity, so that we define ϵ as the non-

[1] See Refs. [11,7,8,12] for more details.

[2] The one with the highest score.

[3] $\overline{R}=\Sigma_{\mu}\rho^{\mu}R^{\mu}$ is the notation for the weighted average over the histories.

[4] See [11]: they are agents that stop being adaptative.

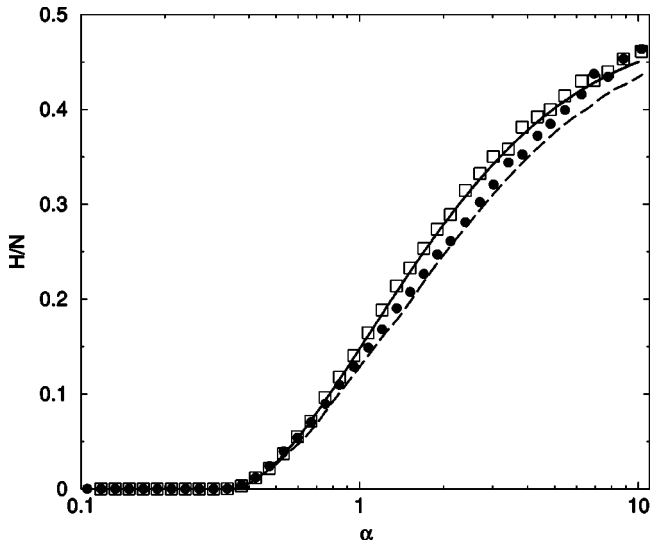

FIG. 4. Comparison between the available information of the MG with uniformly sampled (squares) and real (circles) histories. Dashed and solid lines are corresponding theoretical predictions ($M=8$, $S=2$, $300P$ iterations, average over 200 samples).

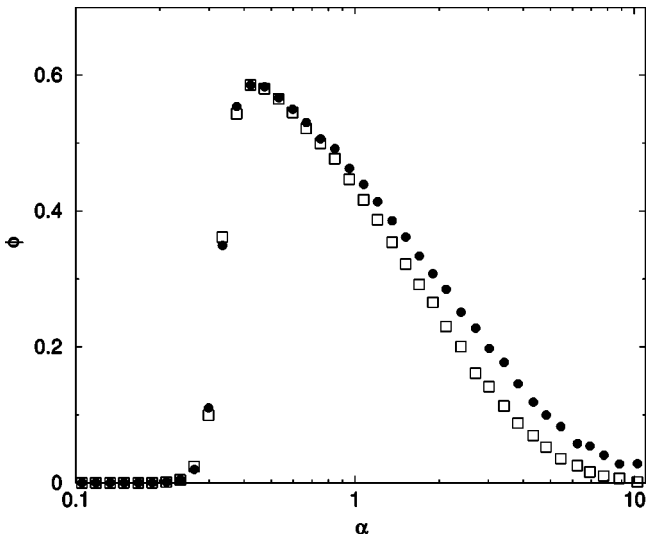

FIG. 5. Comparison between the fraction of frozen agents in the MG with uniformly sampled (squares) and real (circles) histories. In the symmetric phase, these are equal whereas they differ significantly in the asymmetric phase ($M=8$, $S=2$, $300P$ iterations, average over 200 samples).

weighted average[5] of ϵ^μ over the histories. For large P, ϵ can be approximated by

$$\overline{\epsilon}_{th}=2\int_0^\infty dA\,\frac{e^{-A^2/2H}}{\sqrt{2\pi H}}\mathrm{erf}\left(\frac{A}{\sqrt{2(\sigma^2-H)}}\right). \tag{12}$$

Here both H and σ^2 can be computed analytically with the method of Refs. [7,12,8] (see Appendix C). However, the solution depends on the distribution ρ^μ. In order to make Eq. (12) a self-consistent equation for $\overline{\epsilon}_{th}$, we need to parametrize the distribution of ρ^μ by $\overline{\epsilon}_{th}$ itself.

We could not find *ab initio* the analytic form of the PDF of $\{\rho^\mu\}$, but Fig. 7 shows that

$$P(\tau)\simeq\frac{(\lambda+1)^{\lambda+1}}{\Gamma(\lambda+1)}\tau^\lambda e^{-(\lambda+1)\tau} \tag{13}$$

is a very good approximation for the PDF of $\rho=\tau/P$. The parameter λ is easily connected with $\overline{\epsilon}_{th}$:

$$\langle\tau^2\rangle-\langle\tau\rangle^2=\frac{1}{1+\lambda}=P^2\Delta\rho^2\simeq\frac{\overline{\epsilon}_{th}^2}{1-\overline{\epsilon}_{th}^2}, \tag{14}$$

where we used Eq. (10). This gives $\lambda\simeq(1-2\overline{\epsilon}_{th}^2)/\overline{\epsilon}_{th}^2$. Note that this approximation requires $\overline{\epsilon}_{th}<1/\sqrt{2}$.

This turns Eq. (12) into an equation for $\overline{\epsilon}_{th}$, and the theory is self-consistent. Figure 8 reports the measured ϵ and its approximation $\overline{\epsilon}_{th}$. What clearly appears from this figure is that ϵ is far from being negligible, and that $\overline{\epsilon}_{th}$ is a quite good approximation to ϵ.

We can also check the validity of Eq. (10) against the self-consistent theory. Figure 9 shows that Eq. (10) is in good agreement with numerical simulations as long as all histories are visited. Moreover, the approximation $\overline{\epsilon}_{th}$ for ϵ leads to qualitatively similar results, but underestimates $\Delta\rho^2$ because $\overline{\epsilon}_{th}<\epsilon$ (see Fig. 8).

The self-consistent replica calculation for the minority game of Refs. [7,12,8] with the ansatz $\rho=\tau/P$ and τ given by the PDF (13) is discussed in Appendix C. Figures 3 and 4 indicate that analytic predictions are well supported by numerical simulations.

In the asymmetric phase, which is arguably the most relevant and interesting in the MG [8], all quantities of the MG change significantly if one replaces real histories with random uniform histories. A dependence on the frequencies ρ^μ

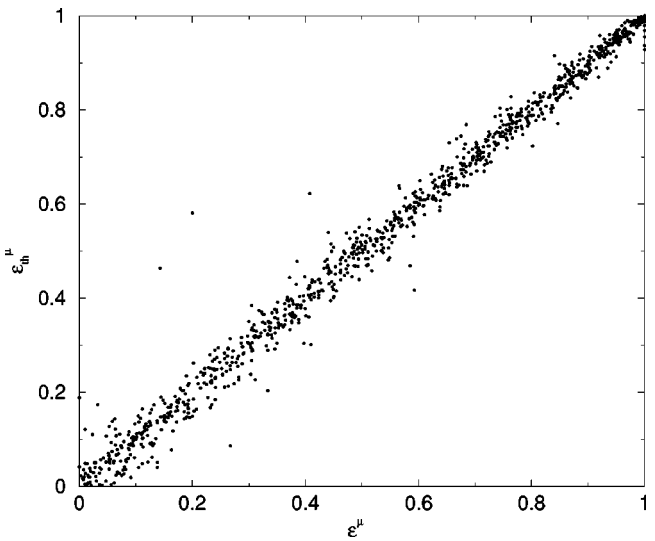

FIG. 6. ϵ_{th}^μ of Eq. (11) vs real ϵ^μ ($M=10$, $N=121$, $S=2$, $1000P$ iterations).

[5]This is clearly an important assumption, but the diffusion on De Bruijn graphs with one ϵ^μ per site leads to a much greater complexity. As appears in Figs. 3, 4, and 9, this assumption is not unrealistic.

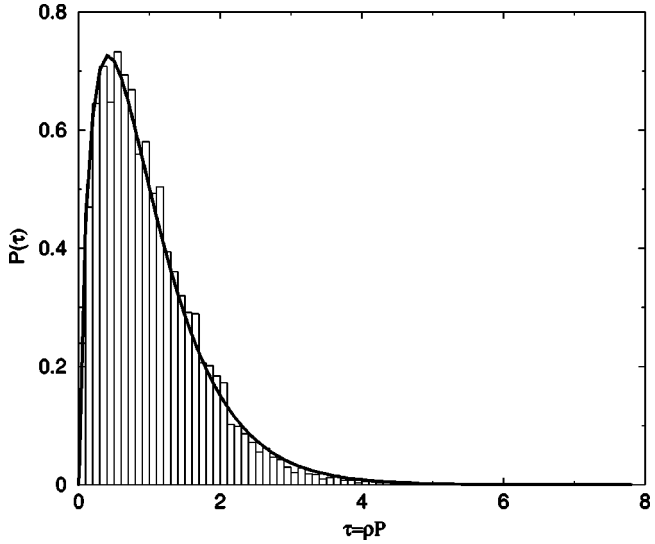

FIG. 7. Distribution of the frequency of visit of the histories in the minority game. The solid line is the best fit for a PDF given by Eq. (13) ($M=13$, $N=801$, $S=2$, $400P$ iterations).

does not necessarily imply the relevance of the detailed dynamics of the histories. If the histories μ where drawn randomly from the ''correct'' distribution ρ^{μ}, the results would be the same (actually it suffices to know the pdf of ρ^{μ}). The problem is that the distribution ρ^{μ} depends on the asymmetry $\langle A^{\mu}\rangle$, which in turn depends on the microscopic constitution of all agents [11]. In other words, ρ^{μ} is a self-consistently determined quantity and hence it is only known *a posteriori*.

VI. CONCLUSION

We have shown that the dynamics of histories cannot be considered as irrelevant. Indeed, even for the canonical MG, it is relevant and cannot be replaced by randomly drawn histories. In addition, for many extensions and variations of the MG, the dynamics of histories is not only relevant, but crucial.

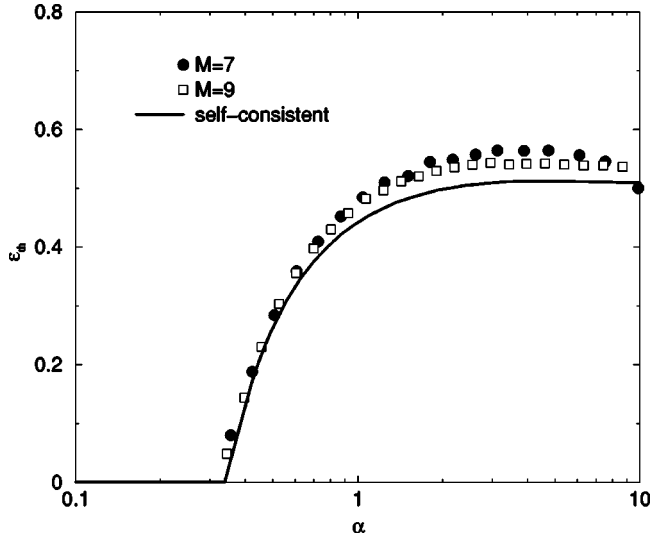

FIG. 8. ϵ versus $\alpha=P/N$ ($M=8$, $S=2$, $300P$ iterations, average over 200 samples). The straight line is $\overline{\epsilon_{th}}$, the theoretical prediction of the self-consistent theory.

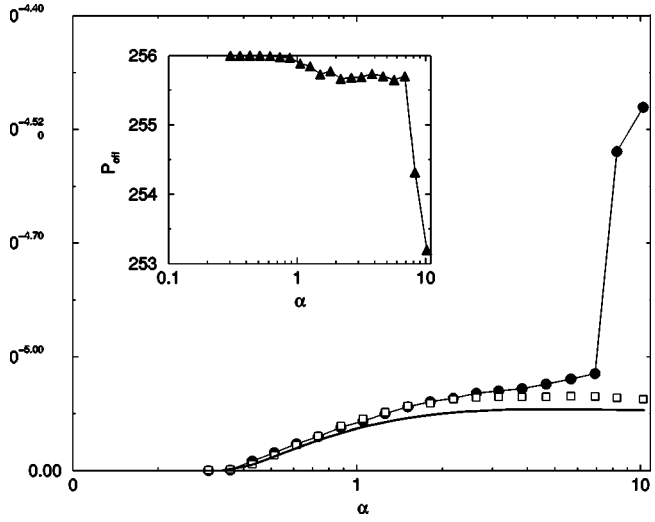

FIG. 9. Inhomogeneity of the frequency of histories $\Delta\rho^2$ versus $\alpha=P/N$ from numerical simulations (circles), Eq. (10) with ϵ from numerical simulations (squares), and Eq. (10) with $\overline{\epsilon_{th}}$ (solid line). Inset: average number of visited histories versus α ($M=8$, $S=2$, $300P$ iterations, average over 200 samples).

ACKNOWLEDGMENTS

We acknowledge fruitful discussions with Philippe Flajolet and Paolo De Los Rios. This work has been partially supported by the Swiss National Science Foundation under Grant No. 20-46918.98.

APPENDIX A

Let us prove by induction that

$$(W_0^k)_{\mu,\nu}=\frac{1}{2^k}\sum_{n=0}^{2^k-1}\delta_{[2^k\mu\%P]+n,\nu}. \tag{A1}$$

It is sufficient to calculate explicitly $(W_0^k)_{\mu,\nu}$ from $(W_0^{k-1})_{\mu,\nu}$,

$$\begin{aligned}(W_0^k)_{\mu,\nu}&=\sum_{\tau=0}^{P-1}(W_0)_{\mu,\tau}(W_0^{k-1})_{\tau,\nu}\\&=\sum_{n=0}^{2^{k-1}-1}\{\delta_{[2^{k-1}([2\mu\%P])\%P]+n,\nu}\\&\quad+\delta_{[2^{k-1}([2\mu\%P]+1)\%P]+n,\nu}\}\\&=\frac{1}{2^k}\sum_{n=0}^{2^k-1}\delta_{[2^k\mu\%P]+n,\nu},\end{aligned} \tag{A2}$$

since $A(B\%P)\%P=AB\%P$ and $(2^k\mu+2^{k-1})\%P=[2^k\mu\%P]+2^{k-1}$ if $P=2^M$ and $k\leqslant M-1$.

APPENDIX B

In order to simplify the notation, we define

$$(X^c)_{\mu,\nu}=\sum_{n=0}^{2^c-1}\delta_{[2^{c+1}\mu\%P]+n,\nu}-\delta_{[2^{c+1}\mu\%P]+n+2^c,\nu}. \tag{B1}$$

This matrix is such that

$$(X^c)_{\mu,\nu}=\begin{cases}1 & \text{if } 2^{c+1}\mu\%P\leqslant\nu<[2^{c+1}\mu\%P]+2^c,\\ -1 & \text{if } [2^{c+1}\mu\%P]+2^c\leqslant\nu<2^{c+1}(\mu+1)\%P,\\ 0 & \text{otherwise.}\end{cases} \tag{B2}$$

With this formalism, one can write W_1V as

$$(W_1V)_{\mu,\nu}=\frac{\xi_\mu}{2}\sum_{c=0}^{M-1}\frac{1}{2^c}(X^c)_{\mu,\nu}. \tag{B3}$$

Let us calculate the perturbation at order 1: one has to compute $||\rho_{(1)}||^2$ in order to have an estimation of the typical value of a generic $\rho^\nu_{(1)}$: since the ξ are uncorrelated and $\Sigma_{\nu=0}^{P-1}(X^c)_{\mu,\nu}(X^d)_{\mu,\nu}=2^{c+1}\delta_{c,d}$,

$$\langle||\rho_{(1)}||^2\rangle_\xi=\frac{1}{4P^2}\sum_{\mu,\nu=0}^{P-1}\sum_{c=0}^{M-1}\frac{[(X^c)_{\mu,\nu}]^2}{2^{2c}}=\frac{(1-1/P)}{P}. \tag{B4}$$

The next orders of perturbation are much harder to handle. However, for large P, one can approximate them by supposing that

$$\langle||\rho_{(k)}||^2\rangle_\xi\sim(1-1/P)\langle||\rho_{(k-1)}||^2\rangle_\xi=\frac{(1-1/P)^k}{P}. \tag{B5}$$

Consequently, $\rho^\nu_{(k)}\sim(1-1/P)^{k/2}(1/P)\simeq 1/P$ at leading order.

APPENDIX C

Since agents actually minimize H/N, one can consider this quantity as a Hamiltonian and find its ground state. This is possible by methods of statistical physics such as the replica trick [13,14]. The generalization of the calculus of Refs. [7,12,8] to $\rho^\mu=\tau^\mu/P$ drawn from the pdf given by Eqs. (13) and (12) is straightforward; the free energy reads, in the thermodynamic limit,

$$F(\beta,Q,q,R,r)=\left\langle\frac{\alpha}{2\beta}\ln[1+\chi\tau]\right\rangle_\tau+\frac{1+q}{2}\left\langle\frac{1}{\frac{1}{\tau}+\chi}\right\rangle_\tau+\frac{\alpha\beta}{2}(RQ-rq)-\frac{1}{\beta}\left\langle\ln\int_{-1}^{1}dse^{-\beta(\zeta s^2-\sqrt{\alpha r}zs)}\right\rangle_z, \tag{C1}$$

where $\chi=\beta(Q-q)/\alpha$ and $\zeta=-\sqrt{\alpha/r}\beta(R-r)$. Next, the $\beta\to\infty$ limit is taken while keeping finite χ and ζ. One obtains

$$H=\frac{1+Q}{2}\left[\left\langle\frac{1}{\frac{1}{\tau}+\chi}\right\rangle_\tau-\chi\left\langle\frac{1}{\left[\frac{1}{\tau}+\chi\right]^2}\right\rangle_\tau\right] \tag{C2}$$

and

$$\sigma^2=H+\frac{1-Q}{2}, \tag{C3}$$

where Q and χ take their saddle point values, given by the solution of

$$Q(\zeta)=1-\sqrt{\frac{2}{\pi}}\frac{e^{-\zeta^2/2}}{\zeta}-\left(1-\frac{1}{\zeta^2}\right)\mathrm{erf}\left(\frac{\zeta}{\sqrt{2}}\right), \tag{C4}$$

$$Q(\zeta)=\frac{1}{\alpha}\left[\frac{\mathrm{erf}(\zeta/\sqrt{2})}{\chi\zeta}\right]^2\frac{1}{\left\langle\frac{1}{[1/\tau+\chi]^2}\right\rangle_\tau}-1, \tag{C5}$$

$$\chi\left\langle\frac{1}{\frac{1}{\tau}+\chi}\right\rangle_\tau=\frac{\mathrm{erf}(\zeta/\sqrt{2})}{\alpha}. \tag{C6}$$

Equations (C5) and (C6), together with Eq. (12), form a closed set of equations that has to be solved numerically. Note that as in the random histories case, χ becomes infinite at the critical point, where $\alpha_c=\mathrm{erf}(\zeta/\sqrt{2})$.

[1] D. Challet and Y.-C. Zhang, Physica A **246**, 407 (1997).

[2] See the minority game's web page on http://www.unifr.ch/econophysics/minority

[3] W.B. Arthur, Am. Econ. Assoc. Papers Proc. **84**, 406 (1994); http://www.santafe.edu/arthur/Papers/El_Farol.html.

[4] A. Cavagna, Phys. Rev. E **59**, R3783 (1999).

[5] N.F. Johnson, P.M. Hui, D. Zheng, and M. Hart, e-print cond-mat/9903164.

[6] N.F. Johnson, M. Hart, P.M. Hui, and D. Zheng, e-print cond-mat/9910072.

[7] D. Challet, M. Marsili, and R. Zecchina, Phys. Rev. Lett. **84**, 1824 (2000).

[8] M. Marsili, D. Challet, and R. Zecchina, Physica A **280**, 522 (2000).

[9] See web page http://www.scs.carleton.ca/~quesnel/papers/debruijn/paper.html for a nice introduction to De Bruijn

graphs.
[10] R. Savit, R. Manuca, and R. Riolo, Phys. Rev. Lett. **82**, 2203 (1999).
[11] D. Challet and M. Marsili, Phys. Rev. E **60**, 6271 (1999).
[12] D. Challet, M. Marsili, and Y.-C. Zhang, Physica A **276**, 284 (2000).
[13] M. Mezard, G. Parisi, and M. A. Virasoro, *Spin Glass Theory and Beyond* (World Scientific, Singapore, 1987).
[14] V. Dotsenko, *An Introduction to the Theory of Spin Glasses and Neural Networks* (World Scientific, Singapore, 1995).